Pergamon

SCIENCE DIRECT®

Tetrahedron 59 (2003) 3833–3844

TETRAHEDRON

A fullerene core to probe dendritic shielding effects

Yannick Rio,[a] Gianluca Accorsi,[b] Hélène Nierengarten,[c] Cyril Bourgogne,[a] Jean-Marc Strub,[c] Alain Van Dorsselaer,[c,*] Nicola Armaroli[b,*] and Jean-François Nierengarten[a,*]

[a]*Groupe des Matériaux Organiques, Institut de Physique et Chimie des Matériaux de Strasbourg, Université Louis Pasteur et CNRS (UMR 7504), 23 rue du Loess, 67034 Strasbourg, France*
[b]*Istituto per la Sintesi Organica e la Reattivitta', Consiglio Nazionale delle Ricerche, via Gobetti 101, 40129 Bologna, Italy*
[c]*Laboratoire de Spectrométrie de Masse Bio-organique, Ecole de Chimie, Polymères et Matériaux (ECPM), Université Louis Pasteur and CNRS (UMR 7509), 67037 Strasbourg, France*

Received 5 November 2002; revised 2 January 2003; accepted 10 January 2003

Abstract—Dendrimers with a C_{60} core have been obtained by cyclization of dendritic bis-malonate derivatives at the carbon sphere. The resulting bis-methanofullerene derivatives have been characterised by electrospray (ES) and/or MALDI-TOF mass spectrometries. UV–VIS absorption spectra, fluorescence spectra, and fullerene singlet excited state lifetimes have been determined in solvents of different polarity (toluene, dichloromethane, acetonitrile). These data suggest a tighter core/periphery contact upon increase of solvent polarity and dendrimer size. In all the investigated solvents, the fullerene triplet lifetimes are steadily increased with the dendrimer volume, reflecting lower diffusion rates of O_2 inside the dendrimers along the series. Measurements of quantum yields of singlet oxygen sensitization indicate that longer lived triplet states generate lower amounts of singlet oxygen ($^1O_2^*$) in dichloromethane but not in apolar toluene suggesting a tighter contact between the dendritic branches and the fullerene core in CH_2Cl_2. In acetonitrile, the trend in singlet oxygen production is peculiar. Effectively, enhanced singlet oxygen production is monitored for the largest dendrimer. This reflects specific interactions of excited $^1O_2^*$ molecules with the dendritic wedges, as probed by singlet oxygen lifetime measurements, possibly as a consequence of trapping effects.

1. Introduction

On account of their fascinating structures and properties, dendrimers have attracted increasing attention in the past few years.[1–18] This interest is mainly related to the capability of a dendritic architecture to generate specific properties. For example, a dendritic framework can surround active core molecules, thus creating specific site-isolated microenvironments capable of affecting the properties of the core itself.[19,20] As part of this research, we have recently shown that dendrimers with a fullerene core are good candidates to demonstrate the shielding effects resulting from the presence of the surrounding dendritic shell.[21] Effectively, the lifetime of the first triplet excited state of fullerene derivatives is very sensitive to the solvent, and lifetime measurements in different solvents can be used to evaluate the degree of isolation of the central C_{60} moiety from external contacts. Even if a dendritic effect was evidenced, the triplet lifetimes of the largest compound investigated in our previous study were found to be rather different in various solvents, likely reflecting specific solvent–fullerene interactions that affect excited state deactivation rates.[21] This suggests that even the largest wedge was not able to provide a complete shielding of the central fullerene core. The latter hypothesis was confirmed by computational studies. As shown in Figure 1, the calculated structure of the largest fullerodendrimer reveals that the dendritic shell is unable to completely cover the fullerene core (the calculations have been performed in the absence of solvent, our aim being only to estimate the possible degree of isolation).

In this paper, we now report a new series of dendrimers with a fullerene core. In the design of compounds **1**–**4**, it was decided to attach two dendritic branches to the C_{60} unit in order to improve the shielding of the central chromophore when compared to our first series of fullerodendrimers. The photophysical properties of **1**–**4** have been systematically investigated in different solvents and revealed that the triplet lifetimes of the largest compound tend towards a similar value. The latter observation suggests that the fullerene core is in a similar environment whatever the nature of the solvent is. In other words the C_{60} core is, to a large extent, not surrounded by solvent molecules but substantially buried in the middle of the dendritic structure. Importantly, the analysis of the trends of triplet lifetimes and singlet oxygen sensitization yields provides some indications of the mechanisms governing the protection of dendrimer cores, a quite elusive goal for a long time.

Keywords: dendrimers; fullerene derivatives; MALDI-TOF; shielding effect; photophysics.

* Corresponding authors. Tel.: +33-388-10-71-63; fax: +33-388-10-72-46; e-mail: niereng@ipcms.u-strasbg.fr; vandors@chimie.u-strasbg.fr; armaroli@isof.cnr.it

0040–4020/03/$ - see front matter
doi:10.1016/S0040-4020(03)00433-2

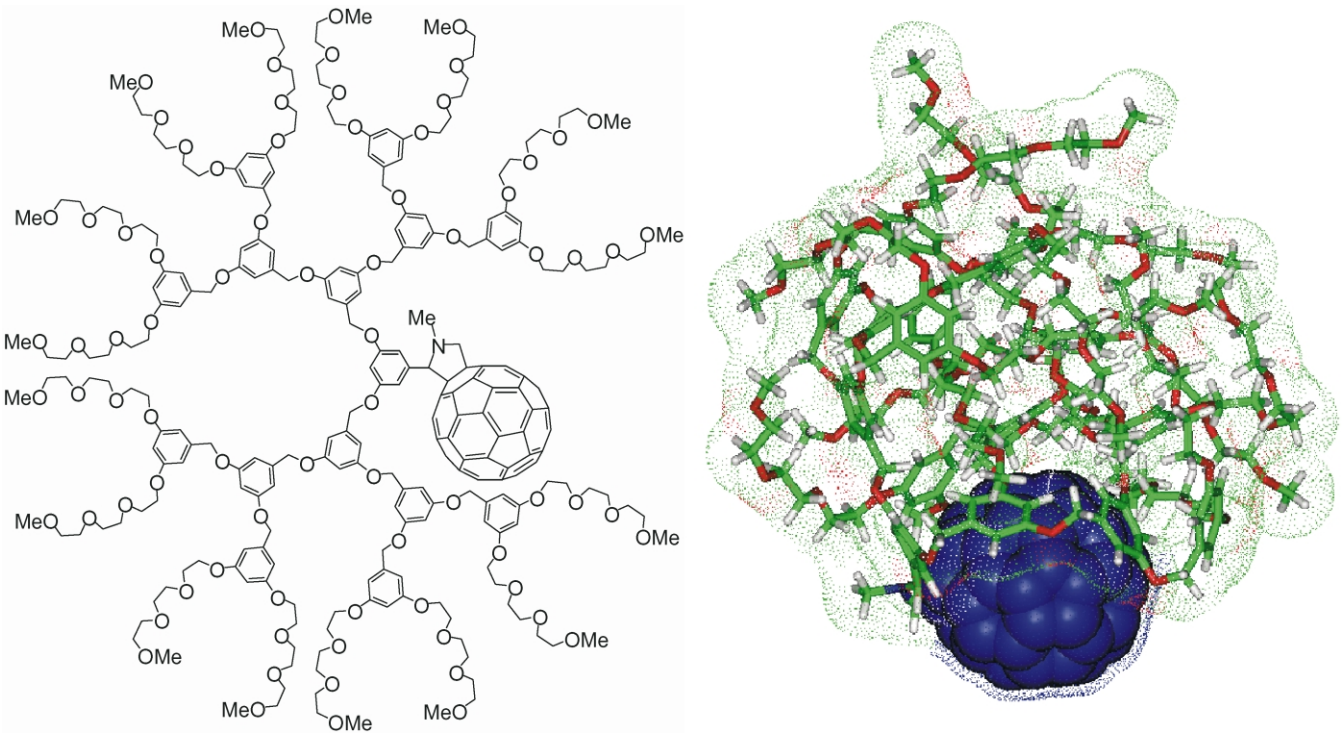

Figure 1. Calculated structure of the largest compound investigated in our previous study.

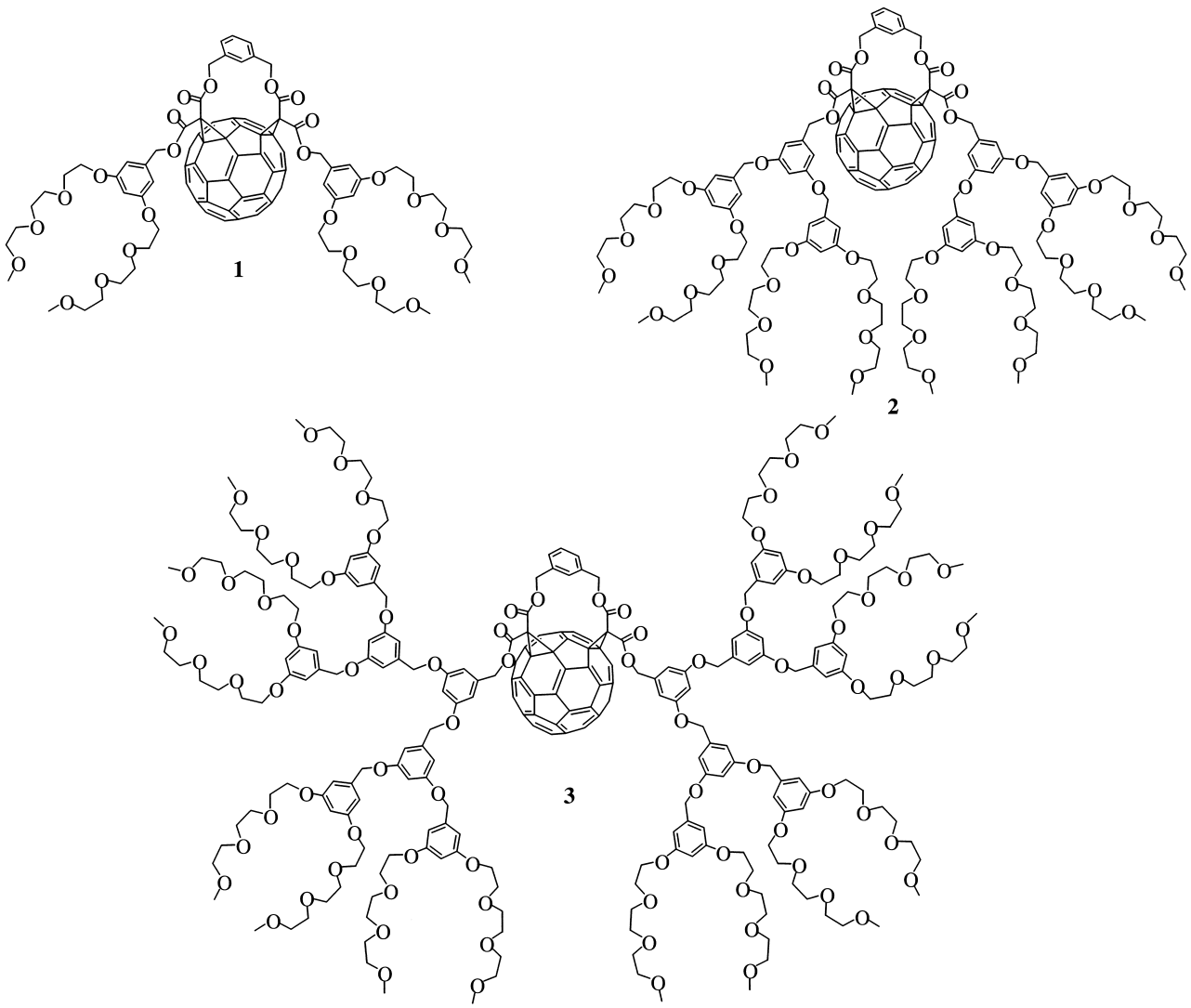

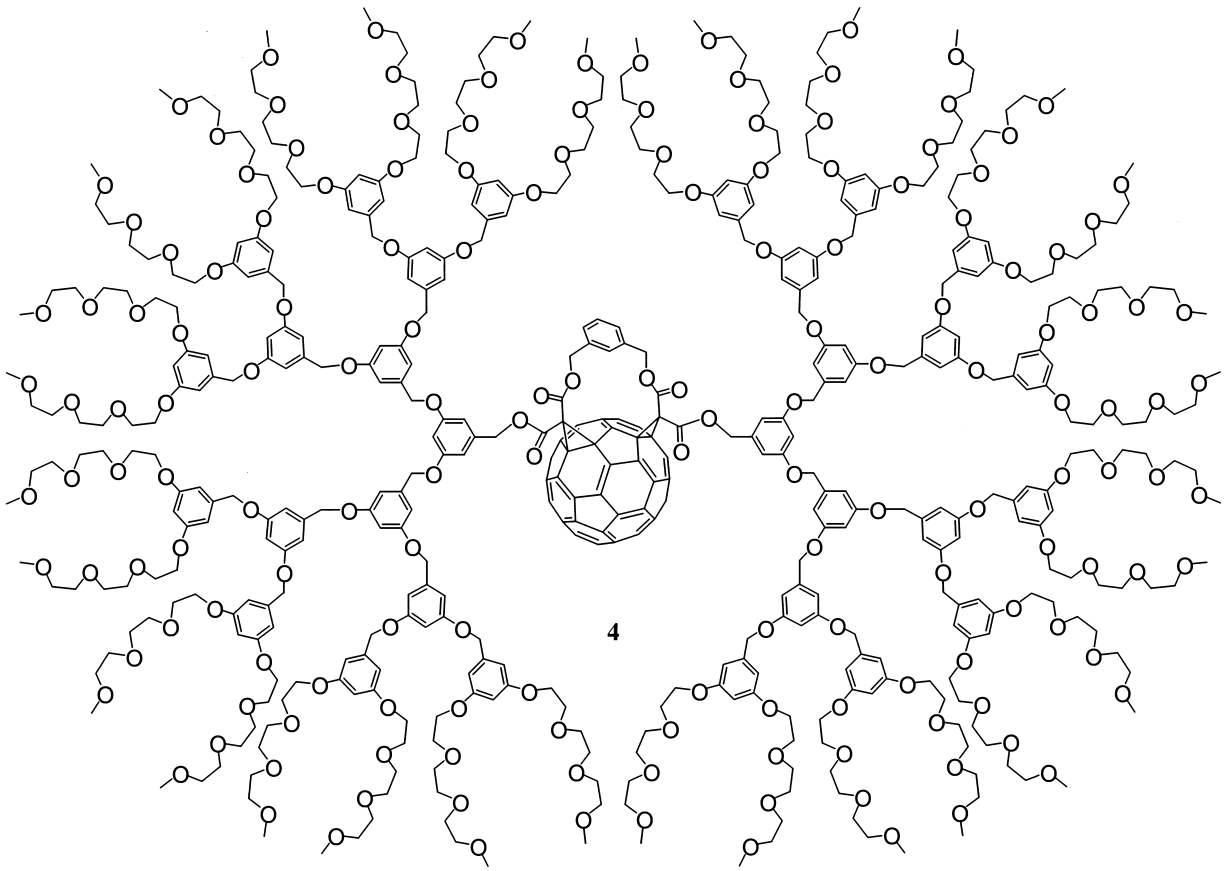

2. Results and discussion

2.1. Synthesis

The preparation of fullerodendrimers **1**–**4** is depicted in Scheme 1. Compound **5**[22] and the triethyleneglycol terminated poly(aryl ether) dendrons **6**–**9**[23,24] have been prepared according to previously reported procedures. *N*,*N*′-Dicyclohexylcarbodiimide (DCC)-mediated esterification of **5** with the dendritic alcohols **6**–**9** in CH_2Cl_2 afforded the corresponding bis-malonates **10**–**13**.

Fullerodendrimers **1**–**4** were then obtained by taking advantage of the versatile regioselective reaction developed in the group of Diederich,[25] which generated macrocyclic bis-adducts of C_{60} by a cyclization reaction at the C sphere with bis-malonate derivatives in a double Bingel cyclopropanation.[26] Reaction of **10**–**13** with C_{60}, I_2, and DBU in toluene at room temperature afforded the corresponding cyclization products **1**–**4**. The relative position of the two cyclopropane rings in **1**–**4** on the C_{60} core was determined based on the molecular symmetry deduced from the ^1H and ^{13}C NMR spectra (C_S). The ^1H NMR spectra of **1** and **2** are depicted in Figure 2. In addition to the signals corresponding to the dendritic branches, both spectra are characterized by two sets of AB quartets for the diastereotopic benzylic CH_2 groups and an AB_2X system for the aromatic protons of the bridging phenyl ring. The UV–VIS spectra of **1**–**4** also show all the characteristic features seen for previously reported analogous *cis*-2 bis-adducts.[22,27–30] It is well established that the absorption spectra of C_{60} bis-adducts are highly dependent on the addition pattern and are characteristic for each regioisomer.[31] In addition, it must also be added that 1,3-phenylenebis(methylene)-tethered bis-malonates regioselectively produce the *cis*-2 addition pattern at C_{60}.[22,27–30]

2.2. Mass spectrometry

The unequivocal characterization of dendrimers also requires their mass spectrometric analysis. Electrospray (ES) and/or matrix-assisted laser desorption/ionization (MALDI) mass spectrometries are the most appropriate tools for such a purpose owing to their gentle ionization processes preventing high levels of fragmentations.[32–34] Compounds **1**–**3** have been characterized by both techniques. As far as ES-MS is concerned, the compounds are uncharged in solutions and their analysis requires the addition of 1% formic acid to charge the fullerene derivatives.[21] For MALDI-MS measurements, several matrices have been tested, such as α-cyanohydroxycinnamic acid, 2,5-dihydrobenzoic acid or 1,8,9-trihydroxyanthracene (dithranol). Singularly, the expected peaks were only detected with dithranol. The ES and MALDI mass spectra of **1** and **2** (not represented here) are all characterized by two singly charged peaks corresponding to the protonated and cation bound (with Na^+) compounds (see Section 4). The mass spectra of **3** are depicted in Figure 3. Both mass spectrometric methods allow the unambiguous characterization of fullerodendrimer **3**. The ES mass spectrum only shows one peak interpreted as $[M+Na^+]$ at m/z=5099.1 (calculated m/z=5098.6).

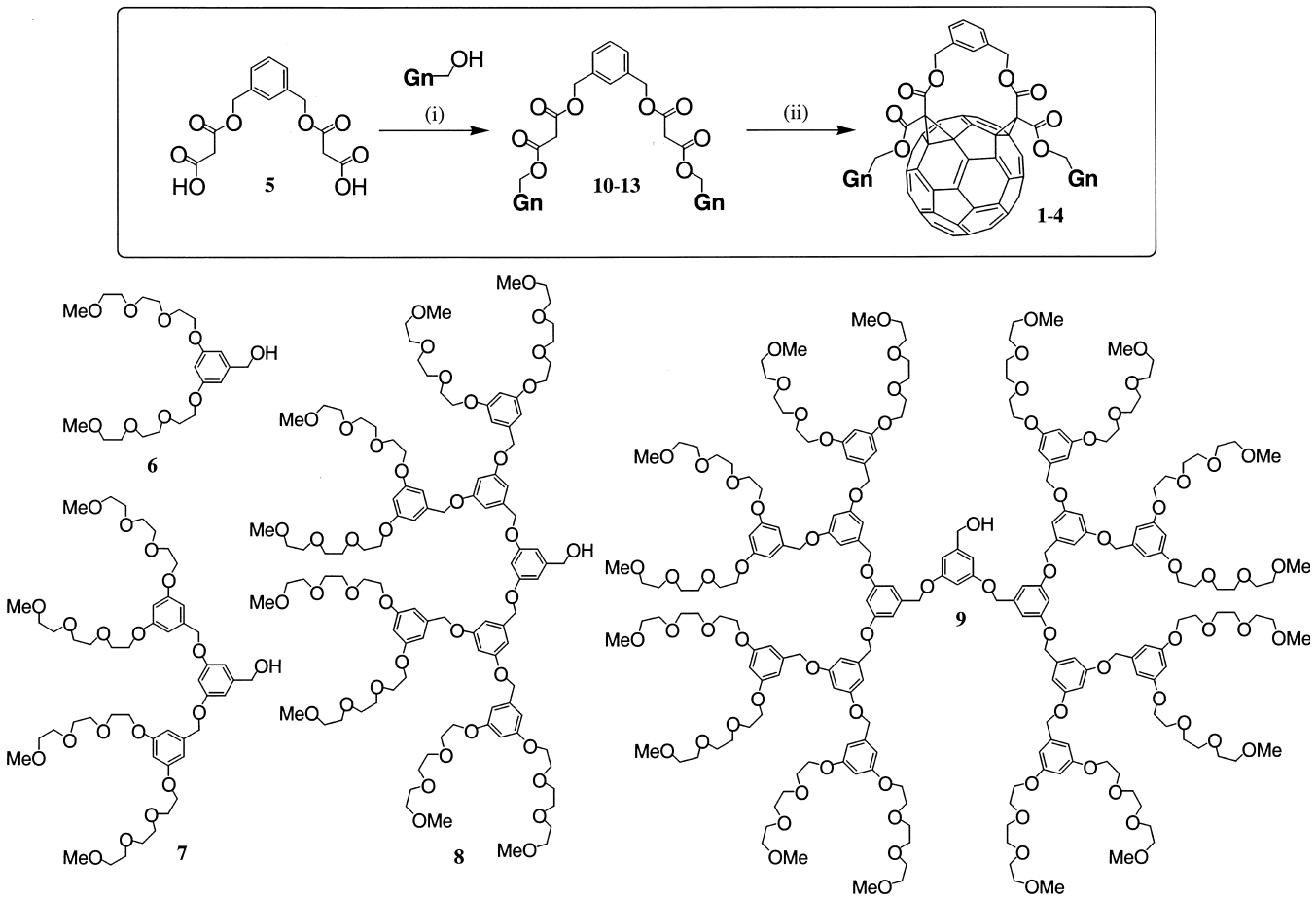

Scheme 1. *Reagents and conditions*: (i) DCC, DMAP, HOBt, CH_2Cl_2, 0 to 25°C, 24 h (**10**: 62%, **11**: 48%, **12**: 49%, **13**: 44%); (ii) C_{60}, I_2, DBU, toluene, room temperature, 24 h (**1**: 25%; **2**: 25%; **3**: 26%; **4**: 24%).

The MALDI mass spectrum shows two peaks interpreted as $[M+H^+]$ at m/z=5076.3 (calculated m/z=5076.6) and as $[M+Na^+]$ at m/z=5098.8 (calculated m/z=5098.6).

Due to the high molecular weight of **4**, its characterization was only possible by MALDI-MS. As a matter of fact, the mass range of our ES instrument (an ES triple quadrupole mass spectrometer with a mass-to-charge (m/z) ratio range

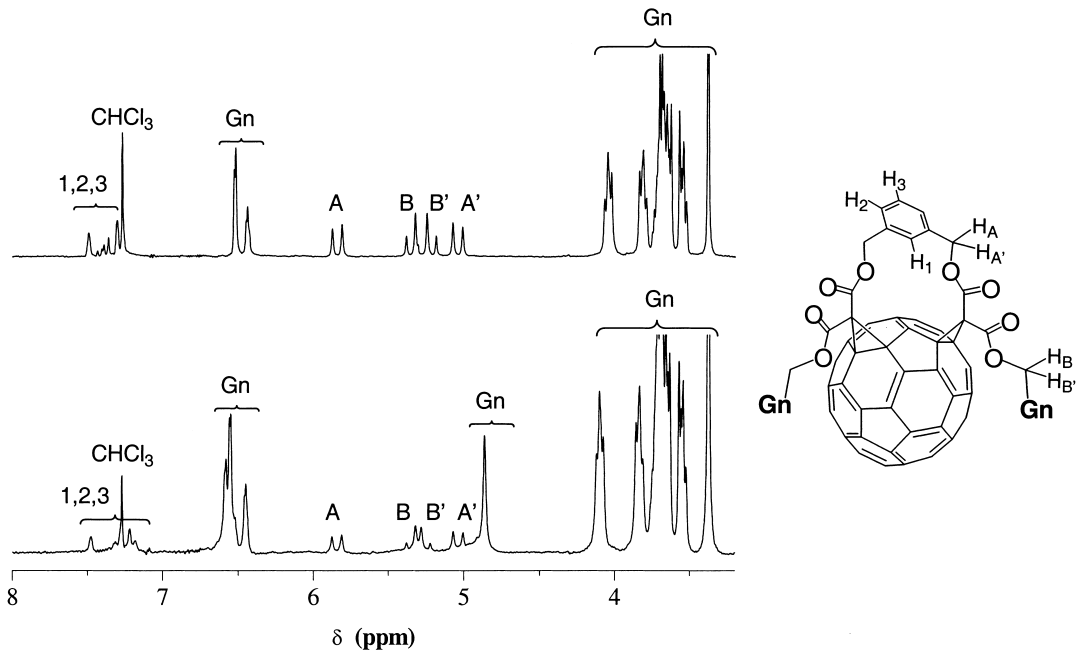

Figure 2. ^1H NMR spectra ($CDCl_3$, 200 MHz) of fullerodendrimers **1** (top) and **2** (bottom).

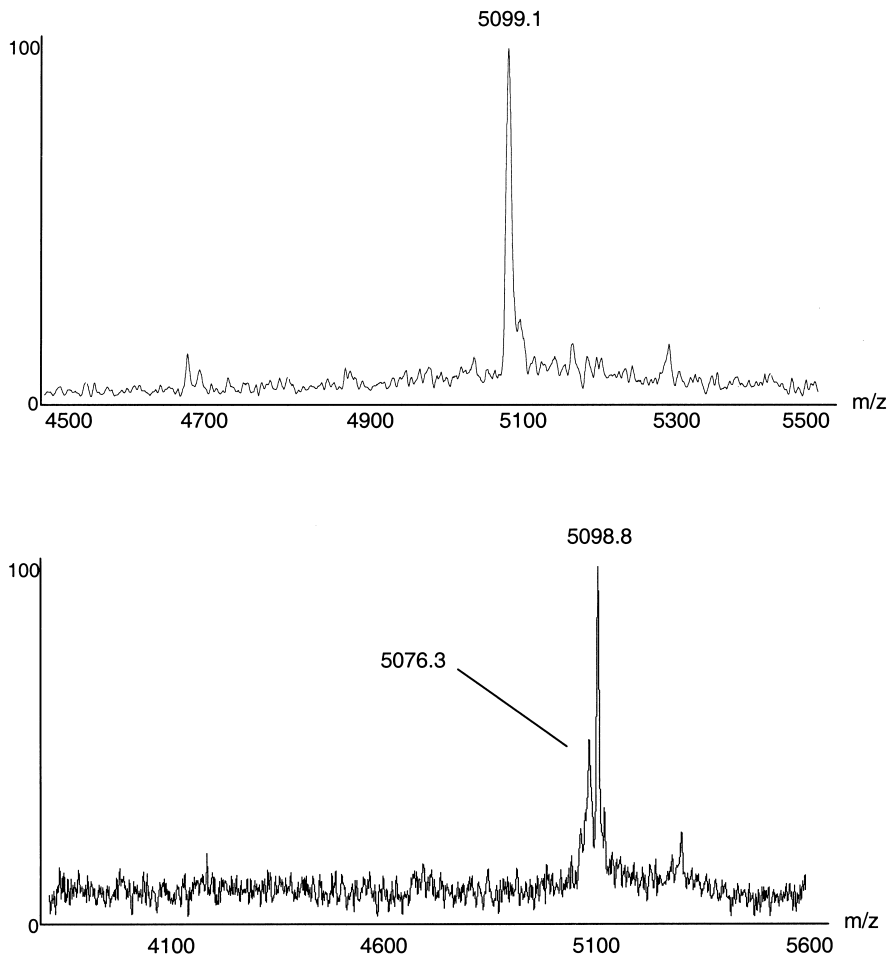

Figure 3. ES (top) and MALDI (bottom) mass spectra of fullerodendrimer **3**.

of 8000) was not sufficient to allow the characterization of **4** (M_W=9391.5). Since, a MALDI mass spectrometer is typically equipped with a time of flight (TOF) analyzer with a theoretically unlimited *m*/*z* range, its use was therefore, an alternative and a complementary method to complete the unambiguous characterization of these compounds. The MALDI mass spectrum of **4** (Fig. 4) presents only one mono-charged peak corresponding to [M+Na^+] at *m*/*z*=9390.0 (calculated *m*/*z*=9391.5).

2.3. Absorption and fluorescence spectra

The UV–VIS absorption spectra of **1**–**4** in toluene, dichloromethane, and acetonitrile ($PhCH_3$, CH_2Cl_2, and CH_3CN, respectively) are reported in Figures 5–7. In CH_2Cl_2 and CH_3CN the increasing contribution of the poly(aryl ether) dendritic branches above 250 and around 280 nm is observed on passing from **1** to **4** (Figs. 6 and 7). Notably, a substantial increase of absorption intensity with

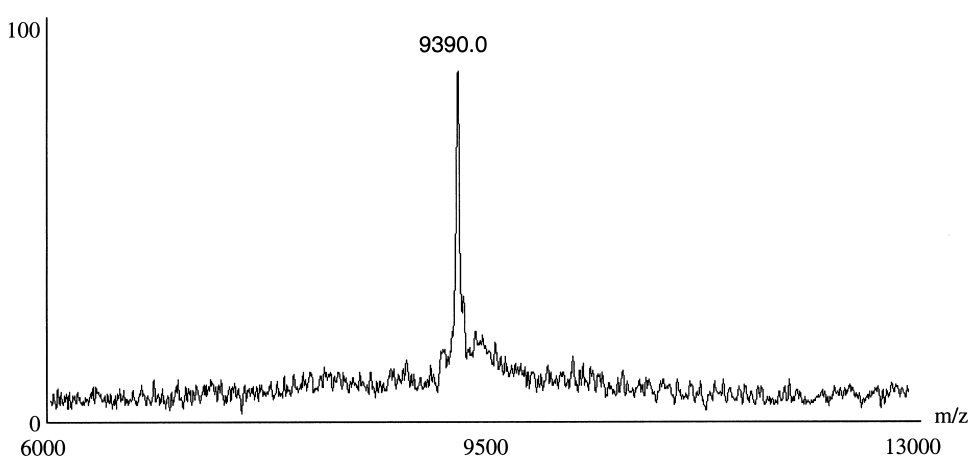

Figure 4. MALDI mass spectrum of fullerodendrimer **4**.

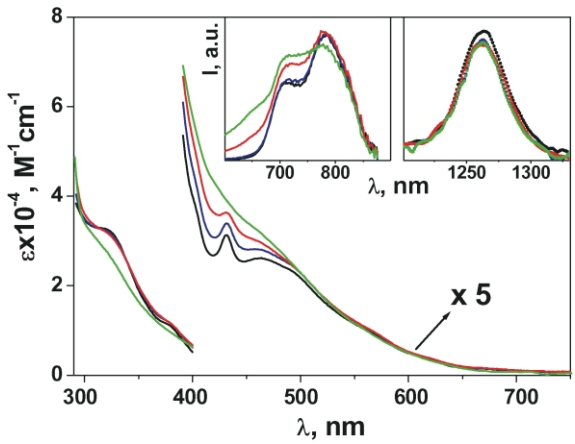

Figure 5. Absorption spectra of **1**–**4** in $PhCH_3$ solution at 298 K; above 400 nm a multiplying factor of 5 is applied. Inset: fluorescence (left, λ_{exc}=370 nm, OD=0.20) and sensitised singlet oxygen luminescence spectra (right, λ_{exc}=480 nm, OD=0.20) of **1**–**4**. **1** (black), **2** (blue), **3** (red), **4** (green).

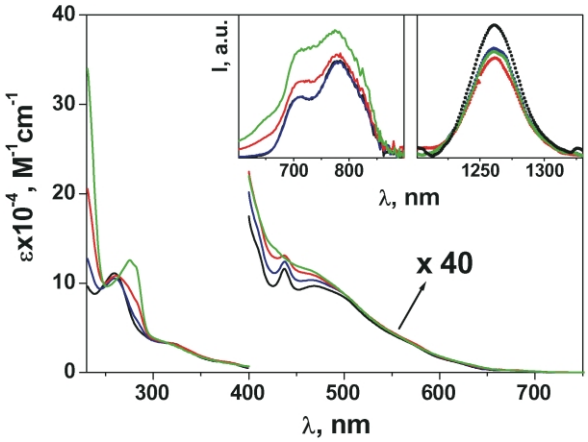

Figure 6. Absorption spectra of **1**–**4** in CH_2Cl_2 solution at 298 K; above 400 nm a multiplying factor of 40 is applied. Inset: fluorescence (left, λ_{exc}=370 nm, OD=0.20) and sensitised singlet oxygen luminescence spectra (right, λ_{exc}=480 nm, OD=0.20) of **1**–**4**. **1** (black), **2** (blue), **3** (red), **4** (green).

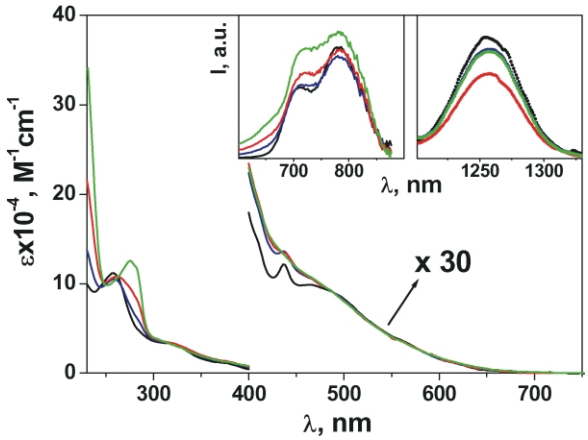

Figure 7. Absorption spectra of **2**–**4** in CH_3CN solution at 298 K; above 400 nm a multiplying factor of 30 is applied. Inset: fluorescence (left, λ_{exc}=370 nm, OD=0.20) and sensitised singlet oxygen luminescence spectra (right, λ_{exc}=480 nm, OD=0.20) of **2**–**4**. **2** (blue), **3** (red), **4** (green). **1** is not soluble in this solvent.

dendrimer generation was recorded in all solvents in the region between 380 and 500 nm. The spectrum of **1**, the smallest representative of the series, was substantially unaffected by change of the solvent polarity throughout the UV–VIS spectral range and is virtually identical to that of other bis-methanofullerenes,[29] showing a diagnostic peak at 438 nm. Thus, we cannot attribute the spectral variations observed upon increase of dendrimer shell to changes of the fullerene/solvent interactions. These changes, instead, can be rationalized by admitting an increasing intramolecular interaction between the fullerene moiety and the external branches, most likely promoted by favourable electronic donor–acceptor attractions.[21] To bring support to this hypothesis we note that the loss of spectral resolution around 438 nm is the fastest, along the series, in polar CH_3CN (Fig. 7), where intramolecular stacking between the dendritic wedges and the hydrophobic central core is expected to be particularly effective. Notably, the trend of absorption spectra is in line with that observed earlier for other families of fullerodendrimers[29,35] and upon complexation of fullerene molecules by dendrimeric hosts.[36]

The fluorescence spectra of **1**–**4** in the three solvents are displayed in Figures 5–7 (inset), and a summary of luminescence data is gathered in Table 1. If compared to fulleropyrrolidines,[21] bismethanofullerenes are even weaker fluorophores.

By increasing the dendrimer size, band broadening is observed in all cases on the high energy side regardless of the excitation wavelength.[37] The largest dendrimer (**4**) exhibits enhanced fluorescence yield in CH_2Cl_2 and CH_3CN (Table 1); its singlet excited state is the longest of the series in any solvent. The slightly different singlet photophysical properties of **4** relative to the smaller analogues can be related to changes in the dendrimer's solvation environment, as a consequence of stronger intramolecular interaction between the core and the dendrons, as suggested above.

As pointed out earlier,[21] the very short singlet lifetime of fullerenes (about 1.5 ns) makes it unsuitable to probe dendritic effects of protection, since intrinsically fast deactivation prevents bimolecular quenching processes. Thus, in order to probe the protection of the fullerene core, it is necessary to investigate the much longer triplet lifetimes (hundreds of ns in air-equilibrated solutions), also taking advantage of the high intersystem crossing yield of methanofullerenes (≥90%).[38]

2.4. Triplet transient absorption spectra and lifetimes

The shape of triplet–triplet transient absorption spectra are substantially identical for **1**–**4** in all the investigated solvents. A wide absorption band peaked at 705 nm is recorded in all cases, as already observed for other bis-methanofullerenes.[29] Triplet lifetime values of the whole family of dendrimers in the three investigated solvents, determined by transient absorption spectroscopy, are gathered in Table 2.

The large difference between a triplet lifetime measured in

Table 1. Fluorescence data and singlet excited state lifetimes at 298 K

	$PhCH_3$			CH_2Cl_2			CH_3CN		
	λ_{max} (nm)[a]	$\Phi\times10^4$	τ (ns)	λ_{max} (nm)[a]	$\Phi\times10^4$	τ (ns)	λ_{max} (nm)[a]	$\Phi\times10^4$	τ (ns)
1	710, 782	4	1.3	710, 780	3	1.4	712, 782	4	1.5
2	712, 782	4	1.4	710, 780	3	1.3	720, 782	4	1.5
3	716, 782	5	1.5	710, 780	4	1.5	720, 782	4	1.5
4	716, 782	5	1.8	710, 776	5	1.8	720, 782	5	1.9

Fluorescence spectra and quantum yields (Φ) were obtained upon excitation at 370 nm; excited state lifetimes upon excitation at 337 nm (see Section 4).
[a] From spectra corrected for the photomultiplier response; highest energy fluorescence peak and band maximum, respectively.

Table 2. Triplet lifetimes as determined by transient absorption at 298 K in air equilibrated (AER) and oxygen-free solutions (DEA) solutions

	$PhCH_3$		CH_2Cl_2		CH_3CN	
	AER (ns)	DEA (μs)	AER (ns)	DEA (μs)	AER (ns)	DEA (μs)
1	288	21.3	611	19.0	314	13.6
2	317	23.0	742	20.0	380	14.7
3	448	26.8	873	25.9	581	20.0
4	877	34.7	1103	31.7	1068	27.9

air equilibrated (AER) vs air-free solution (DEA) is attributable to the very efficient oxygen quenching undergone by C_{60} fullerenes (see below).[39] On the other hand the differences found for **1** (the reference bismethanofullerene) in different solvents are typical for C_{60}'s and indicate that solvent interactions strongly affect the deactivation rate constants of fullerene excited states.

For **1**–**4** a steady prolongation of air-equilibrated triplet lifetimes is found by increasing the dendrimer's size in all solvents (Table 2). Since the fullerene active core is absolutely identical along the series, one has to conclude that dendritic wedges are able to partially shield the fullerene core from interactions with dioxygen molecules.

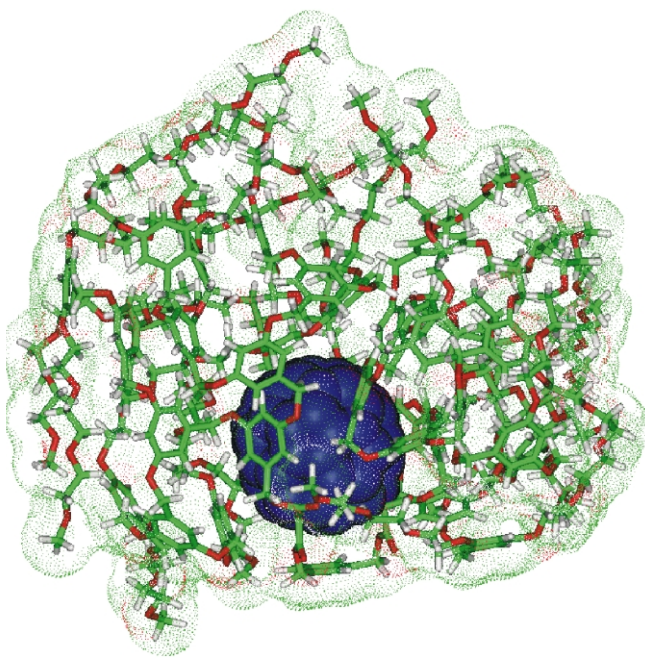

Figure 8. Snapshot of the theoretical structure of the largest fullerodendrimer **4** at 300 K obtained from a Molecular Dynamics calculation.

Similar protective effects towards dioxygen quenching have been already observed for other dendrimer cores exhibiting long lived electronic excited states.[21,40–42]

By inspecting the data of air-equilibrated triplet lifetimes in Table 2 some trends can be emphasized. For instance, although the lifetime of **1** is substantially different in CH_2Cl_2 and CH_3CN (611 and 314 ns, respectively) an identical lifetime, within experimental uncertainties, is measured for **4** (≈1100 ns). This suggests that in CH_2Cl_2 and CH_3CN the fullerene core of **4** is buried inside the dendritic cage, and has negligible interactions with the solvent molecules. Notably, in toluene and CH_3CN the lifetime of **1** is shorter than in CH_2Cl_2, but in both solvents an increase of over 200% is observed for **4**, pointing to a very effective shielding of the dendritic cage in solvents of any polarity.

The data presented here can be usefully compared to those obtained for fullerodendrimers with a fulleropyrrolidine core and similar dendritic branches; the largest representative of which is depicted in Figure 1. In that case, a much less marked lifetime increase was observed on passing from the smallest to the largest dendrimer (only 34% in toluene, for instance), pointing to a much less effective protection of the fullerene active core relative to the present case. This difference can be intuitively rationalized by comparing the structure of **4** with that of the fulleropyrrolidine dendrimer depicted in Figure 1. When the dendritic moiety is anchored at two different points of the carbon sphere, as in **4**, a more effective encapsulation can be reasonably expected in comparison to fulleropyrrolidine analogues. The structure of **4** obtained by molecular modeling supports this hypothesis well (Fig. 8) since it reveals a fullerene core completely buried inside the dendronic external cage, unlike the fulleropyrrolidine analogue, where the core is still partially exposed to external contacts (Fig. 1).

Triplet lifetimes in oxygen-free solutions are also constantly increased by enlarging the dendrimers size, regardless of the solvent (Table 2). Hence, molecular oxygen is not the only potential quencher of fullerene triplet states in solution. This result is not surprising since long-lived triplet states are known to be quenched by solvent impurities such as stabilizers and/or paramagnetic ions,[43] that are commonly present in not negligible amounts in spectroscopic grade solvents. This trend in triplet lifetimes of air-purged samples is taken as a further proof of a protective dendritic effect along the series **1**–**4**. Notably, in fullerodendrimers with more rigid dendrons no prolongation of triplet lifetimes has been observed.[44,45]

The less effective quenching of fullerene triplet states by increasing the dendrimer size can be assigned to one or more of the following factors: (a) decrease in the diffusion rate of O_2 inside the peripheral wedges, with increasing the molecular volume; (b) lower solubility of O_2 in the interior of the dendrimers; (c) preferential solvation of the C_{60} core by the dendrimer branches, hindering suitable orbital overlap for singlet oxygen sensitization. The data and discussion below will help us to obtain a better picture of the quenching mechanism of the dendrimer core.

2.5. Singlet oxygen sensitization

The quenching of C_{60} fullerene triplet states in solution by molecular oxygen is due to a triplet–singlet energy transfer process,[39] according to the following reaction scheme:

$$C_{60} \xrightarrow{h\nu} {}^1C_{60}^* \xrightarrow{\text{i.s.c.}} {}^3C_{60}^* \xrightarrow{O_2} C_{60} + {}^1O_2^* \quad (1)$$

where i.s.c. denotes singlet ($^1C_{60}^*$) to triplet ($^3C_{60}^*$) intersystem crossing, and $^1O_2^*$ stands for $O_2(^1\Delta_g)$, commonly named 'singlet oxygen'. The quantum yield of singlet oxygen sensitization (Φ_Δ) is dependent on three parameters: (i) the quantum yield of triplet formation (Φ_T), (ii) the ratio of the sum of triplet decays involving oxygen over the overall triplet decays (S_Q); (iii) the fraction of triplet molecules quenched by oxygen and leading to singlet oxygen (S_Δ):

$$\Phi_\Delta = \Phi_T S_Q S_\Delta \quad (2)$$

in the case of C_{60}, C_{70} and functionalized fullerenes it can be safely assumed that $S_\Delta = S_Q = 1$,[46,47] therefore, $\Phi_\Delta = \Phi_T$ with excellent approximation.[48]

There are several experimental methods to determine Φ_Δ.[49] A relatively simple one involves monitoring the $^1O_2^*$ luminescence band centered at 1270 nm under steady-state irradiation for both the sample of interest (x) and a suitable reference standard sample (st), for which Φ_Δ is known.[49] The unknown Φ_Δ value can be determined by means of Eq. (3):[50]

$$\Phi_\Delta^x = \Phi_\Delta^{st} \frac{I_x(1-10^{-A})_{st}}{I_{st}(1-10^{-A})_x} \frac{n_x^2}{n_{st}^2} \frac{k_r^{st}}{k_r^x} \quad (3)$$

where I is the luminescence intensity at the emission maximum (1270 nm), A the absorbance, n the solvent refractive index, and k_r the dioxygen radiative rate constant of deactivation, which is strongly solvent dependent.[51,52] By working in the same solvent and with optically matched solutions Eq. (3) is simplified into Eq. (4):

$$\Phi_\Delta^x = \Phi_\Delta^{st} \frac{I_x}{I_{st}} \quad (4)$$

In Figures 5–7 (inset) are reported the relative emission intensities of the sensitized singlet oxygen emission bands taken under the same experimental conditions for each solvent. Comparisons between spectra in different solvents cannot be made since, both radiative[51,52] and non-radiative[53] deactivations of singlet oxygen are extremely solvent dependent.

In toluene, as derived from luminescence band intensities in the NIR region (Fig. 5), the relative quantum yield of singlet oxygen sensitization for **1**–**4** is substantially unchanged along the series. Surprisingly, at the same time, triplet lifetimes of the sensitizer are dramatically increased in parallel with the dendrimer dimensions. These results indicate that, along the **1**–**4** series, the sensitization process is simply delayed but finally leads to the same result, i.e. quantitative sensitization of singlet oxygen regardless of the dendrimer size. The observed trend suggests that the role of the dendritic branches is that of delaying the quenching process but not of hindering it. Such a trend can be rationalized by considering a decrease in the diffusion rate constant of O_2 inside the dendrimer wedges with increasing volume of the compound (see above). Once O_2 has reached the dendrimer surface, however, effective $O_2/^3C_{60}^*$ orbital overlap can still take place, followed by singlet–triplet energy transfer (Eq. (1)).

In CH_2Cl_2, the lifetime trend is similar to that in toluene, but the yield of singlet oxygen formation is sizeably depressed for **2**–**4** relative to **1**. The delayed quenching can be explained by the same arguments as in toluene, whereas the decrease of singlet oxygen yield may be due to tighter contacts between the periphery and the core, which hinder suitable orbital overlap between the carbon cage and dioxygen.[40] This is in line with the results of the absorption and luminescence spectra.

In the most polar medium, CH_3CN, the trend in singlet oxygen production is peculiar. A progressive decrease (up to 30%) is detected from **1** to **3**. This can be explained with the rationale outlined for CH_2Cl_2, the more pronounced decrease of singlet oxygen generation being ascribable to an even tighter core/periphery contact in polar CH_3CN. Quite unexpectedly, a recovery of singlet oxygen production is found for the largest dendrimer **4**. This effect is difficult to explain, however, it might reasonably be due to specific effects on the quantum yield of singlet oxygen luminescence Φ_L, which is given by Eq. (5):[54]

$$\Phi_L = \Phi_\Delta \frac{k_r}{k_r + k_{nr}} = \Phi_\Delta k_r \tau \quad (5)$$

where k_r, k_{nr}, and τ are the radiative and non-radiative deactivation rate constants and lifetimes of singlet oxygen, respectively.

To test this hypothesis we have performed lifetime measurements of singlet oxygen in different solvents, in order to see if there is any difference for the various dendrimers. As pointed out earlier, the lifetime of singlet oxygen is dramatically solvent dependent since, both k_r[51,52] and k_{nr}[53] are affected (to a different extent) by the solvent nature. In particular enhanced lifetime values are measured in deuterated solvents.[49]

Identical values for the whole **1**–**4** series were measured in toluene (21±2 μs), deuterated toluene (280±28 μs), and CH_2Cl_2 (120±12 μs). These results are in line with literature data in the same solvents[49] and suggest that there is no trapping effects of oxygen inside the dendrimers cage in low-polarity and mid-polarity solvents. In other

words, the long lived singlet oxygen experiences the bulk solvent environment.

The results in acetonitrile, however, are interestingly different. For **1**–**3** we measure τ=67±6 μs (typical for this solvent),[49] whereas for **4** τ=33±3 μs. This shows that the k_r and k_{nr} values of $^1O_2$ are substantially modified in **4**, suggesting that $^1O_2^*$ could even be trapped inside the tight dendrimer cage which is formed in polar media. Such subtle effects on the deactivation rates of singlet oxygen could result in unexpected effects on the patterns of luminescence intensity, when the dendrimer's structure becomes bigger.

3. Conclusions

Analysis of the steady state and time resolved photophysical properties of bismethanofullerenes **1**–**4** have given some insight into the shielding effect exerted by the dendrimer wedges toward the photoactive fullerene core. Regardless of the solvent polarity, the increase in size of the peripheral branches leads to a decrease of dioxygen diffusion rates to the fullerene core, as signalled by an increase of fullerene triplet lifetimes. Triplet quenching by dioxygen, albeit progressively delayed along the series, is nevertheless quantitative for **1**–**4** in toluene as shown by the yields of singlet oxygen sensitization. On the contrary, in more polar dichloromethane and acetonitrile, delayed fullerene triplet quenching is accompanied by a decrease of singlet oxygen sensitization yields. We attribute this effect to a tighter contact, in more polar media, between the peripheral branches and the hydrophobic C_{60} core, that leads to less effective orbital overlap between the quencher (O_2) and the sensitizer (C_{60}).

Polarity effects capable of compacting dendrimer structures can also be derived by steady state absorption and luminescence spectra. Identical triplet lifetimes of **4** in CH_2Cl_2 and CH_3CN (1100 ns), as compared to 877 ns in toluene, bring further support to this hypothesis pointing to a looser structure of **4** in the apolar medium. Notably, for **4**, the singlet oxygen lifetime and sensitization efficiency suggest that trapping effects may become important in polar acetonitrile, when the dendrimer is sufficiently large.

It must be emphasized that the increase of fullerene triplet lifetimes with dendrimer generation is more pronounced in the present case than for a series of fulleropyrrolidine analogues investigated earlier.[21] Thus, by using a bismethanofullerene core we have now achieved a better encapsulation of the C_{60} unit. This conclusion is nicely corroborated by molecular modeling.

4. Experimental

4.1. General

Reagents and solvents were purchased as reagent grade and used without further purification. THF was distilled over sodium benzophenone ketyl. Compounds **5**[22] and **6**–**9**[24] were prepared as previously reported. All reactions were performed in standard glassware under an inert Ar atmosphere. Evaporation and concentration were done at water aspirator pressure and drying in vacuo at 10^{-2} Torr. Column chromatography: silica gel 60 (230–400 mesh, 0.040–0.063 mm) was purchased from E. Merck. Thin Layer Chromatography (TLC) was performed on glass sheets coated with silica gel 60 F_{254} purchased from E. Merck, visualization by UV light. IR spectra (cm^{-1}) were measured on an ATI Mattson Genesis Series FTIR instrument. NMR spectra were recorded on a Bruker AC 200 with solvent peaks as reference. Elemental analyses were performed by the analytical service at the Institut Charles Sadron, Strasbourg.

4.2. General procedure for the synthesis of dendritic bismalonates 10–13

DCC (2.2 equiv.) was added to a stirred solution of **5** (1 equiv.), the appropriate dendritic alcohol (2 equiv.), HOBt (0.1 equiv.) and DMAP (0.5 equiv.) in CH_2Cl_2 at 0°C. After 1 h, the mixture was allowed to slowly warm to room temperature (within 1 h), then stirred for 24 h, filtered and evaporated. The crude product was then purified as outlined in the following text.

4.2.1. Compound 10. Prepared from **6** and purified by column chromatography (SiO_2, CH_2Cl_2/Acetone 4:1) to give **10** as a colourless glassy product which was used without further purification: yield 62%; ^1H NMR ($CDCl_3$, 200 MHz): δ 3.38 (s, 12H), 3.48 (s, 4H), 3.52–3.76 (m, 32H), 3.83 (t, *J*=5 Hz, 8H), 4.09 (t, *J*=5 Hz, 8H), 5.09 (s, 4H), 5.17 (s, 4H), 6.45 (t, *J*=2 Hz, 2H), 6.49 (d, *J*=2 Hz, 4H), 7.32 (broad s, 4H).

4.2.2. Compound 11. Prepared from **7** and purified by column chromatography (SiO_2, CH_2Cl_2/Acetone 7:3) to give **11** as a colourless glassy product which was used without further purification: yield 48%; ^1H NMR (Acetone-d_6, 200 MHz): δ 3.25 (s, 24H), 3.41–3.64 (m, 84H), 4.10 (t, *J*=5 Hz, 16H), 4.99 (s, 8H), 5.10 (s, 4H), 5.15 (s, 4H), 6.46 (m, 6H), 6.62 (m, 12H), 7.31–7.38 (m, 4H).

4.2.3. Compound 12. Prepared from **8** and purified by column chromatography (SiO_2, CH_2Cl_2/Acetone 3:2) to give **12** as a colourless glassy product which was used without further purification: yield 49%; ^1H NMR ($CDCl_3$, 200 MHz): δ 3.37 (s, 48H), 3.47–3.90 (m, 164H), 4.11 (t, *J*=5 Hz, 32H), 4.95 (m, 24H), 5.12 (s, 4H), 5.15 (s, 4H), 6.44 (m, 12H), 6.54 (m, 2H), 6.59 (m, 24H), 6.67 (m, 4H), 7.40 (broad s, 4H).

4.2.4. Compound 13. Prepared from **9** and purified by column chromatography (SiO_2, Et_2O/Acetone 7:3) to give **13** as a colourless glassy product: yield 44%; ^1H NMR (Acetone-d_6, 200 MHz): δ 3.24 (s, 96H), 3.39–4.10 (m, 388H), 4.80–5.10 (m, 64H), 6.40–6.70 (m, 90H), 7.30 (m, 4H).

4.3. General procedure for the synthesis of fullerodendrimers 1–4

DBU (4 equiv.) was added to a stirred solution of C_{60} (1 equiv.), I_2 (3 equiv.) and the appropriate dendritic bismalonate (1 equiv.) in toluene (2 mL/mg of C_{60}). The

resulting solution was stirred for 24 h, then filtered through a short plug of SiO_2, eluting first with toluene (to remove unreacted C_{60}) and then with CH_2Cl_2/8% MeOH. The crude product was then purified as outlined in the following text.

4.3.1. Fullerodendrimer 1. Prepared from **10** and purified by column chromatography (SiO_2, CH_2Cl_2/Acetone 3:2) followed by gel permeation chromatography (Biorad, Biobeads SX-1, CH_2Cl_2) to give **1** as an orange-red glassy product: yield 25%; ^{1}H NMR ($CDCl_3$, 200 MHz): δ 3.38 (s, 12H), 3.53–3.79 (m, 32H), 3.81 (t, J=5 Hz, 8H), 4.05 (t, J=5 Hz, 8H), 5.04 (d, J=13 Hz, 2H), 5.21 (d, J=12 Hz, 2H), 5.36 (d, J=12 Hz, 2H), 5.85 (d, J=13 Hz, 2H), 6.44 (t, J=2 Hz, 2H), 6.52 (d, J=2 Hz, 4H), 7.26–7.49 (m, 4H). ^{13}C NMR ($CDCl_3$, 50 MHz): δ 59.03, 67.40, 67.52, 68.51, 69.61, 70.55, 70.63, 70.79, 71.90, 101.86, 107.41, 123.85, 126.80, 128.62, 135.82, 136.17, 136.68, 140.02, 141.02, 141.18, 142.33, 142.76, 143.18, 143.61, 143.78, 143.99, 144.20, 144.36, 144.61, 144.93, 145.04, 145.20, 145.38, 145.62, 145.75, 146.08, 147.32, 147.48, 148.63, 160.00, 162.53. MALDI-TOF MS: 1856.7 ([M+H]$^+$ calculated for $C_{116}H_{79}O_{24}$: 1856.9, 50%), 1878.6 ([M+Na$^+$] calculated for $C_{116}H_{78}O_{24}Na$: 1878.9, 100%). Elemental analysis calculated for $C_{116}H_{78}O_{24}\cdot H_2O$: C 74.34%, H 4.31%, found: C 74.28%, H 4.57%.

4.3.2. Fullerodendrimer 2. Prepared from **11** and purified by column chromatography (SiO_2, CH_2Cl_2/Acetone 1:1) followed by gel permeation chromatography (Biorad, Biobeads SX-1, CH_2Cl_2) to give **2** as an orange-red glassy product: yield 25%; ^{1}H NMR ($CDCl_3$, 200 MHz): δ 3.38 (s, 24H), 3.53–3.72 (m, 64H), 3.84 (t, J=5 Hz, 16H), 4.10 (t, J=5 Hz, 16H), 4.86 (s, 8H), 5.04 (d, J=13 Hz, 2H), 5.26 (d, J=12 Hz, 2H), 5.35 (d, J=12 Hz, 2H), 5.85 (d, J=13 Hz, 2H), 6.45–6.58 (m, 18H), 7.10–7.48 (m, 4H). ^{13}C NMR ($CDCl_3$, 50 MHz): δ 59.01, 67.47, 68.48, 69.62, 69.99, 70.53, 70.61, 70.77, 71.89, 101.17, 102.29, 106.18, 107.60, 123.68, 126.77, 128.64, 135.72, 136.04, 136.57, 138.87, 138.74, 140.02, 140.96, 141.15, 142.30, 142.73, 143.13, 143.54, 143.74, 143.96, 144.12, 144.28, 144.53, 144.85, 145.00, 145.30, 145.57, 145.71, 146.05, 147.40, 148.62, 159.95, 160.04, 162.50. MALDI-TOF MS: 2930.0 ([M+H]$^+$ calculated for $C_{172}H_{159}O_{44}$: 2930.1, 40%), 2951.9 ([M+Na]$^+$ calculated for $C_{172}H_{158}O_{44}Na$: 2952.1, 100%). Elemental analysis calculated for $C_{172}H_{158}O_{44}$: C 70.52%, H 5.44%, found: C 70.76%, H 5.36%.

4.3.3. Fullerodendrimer 3. Prepared from **12** and purified by column chromatography (SiO_2, CH_2Cl_2/Acetone 1:1) followed by gel permeation chromatography (Biorad, Biobeads SX-1, CH_2Cl_2) to give **3** as an orange-red glassy product: yield 26%; ^{1}H NMR ($CDCl_3$, 200 MHz): δ 3.38 (s, 48H), 3.53–3.72 (m, 128H,), 3.84 (t, J=5 Hz, 32H), 4.11 (t, J=5 Hz, 32H), 4.88 (s, 8H), 4.94 (s, 16H), 5.04 (d, J=13 Hz, 2H), 5.30 (AB, J=12 Hz, 4H), 5.83 (d, J=13 Hz, 2H), 6.45–6.58 (m, 42H), 7.10–7.50 (m, 4H). RMN-^{13}C ($CDCl_3$, 50 MHz): δ 58.99, 67.48, 69.64, 70.01, 70.53, 70.61, 70.79, 71.90, 101.16, 101.64, 106.15, 106.57, 107.62, 123.63, 126.79, 128.65, 135.77, 136.08, 136.58, 136.95, 138.87, 138.95, 140.00, 140.96, 141.17, 142.27, 142.78, 143.16, 143.53, 143.72, 143.94, 144.09, 144.09, 144.24, 144.48, 144.85, 145.01, 145.27, 145.54, 145.70, 146.02, 147.39, 148.60, 160.08. MALDI-TOF MS: 5076.3 ([M+H]$^+$ calculated for $C_{284}H_{319}O_{84}$: 5076.6, 40%), 5098.8 ([M+Na$^+$] calculated for $C_{284}H_{318}O_{84}Na$: 5098.6, 100%). Elemental analysis calculated for $C_{284}H_{318}O_{84}$: C 67.19%, H 6.32%, found: C 67.07%, H 6.29%.

4.3.4. Fullerodendrimer 4. Prepared from **13** and purified by column chromatography (SiO_2, CH_2Cl_2/MeOH 95:5) followed by gel permeation chromatography (Biorad, Biobeads SX-1, CH_2Cl_2) to give **4** as an orange-red glassy product: yield 24%; ^{1}H NMR (Acetone-d_6, 200 MHz): δ 3.23 (s, 96H), 3.24–3.73 (320H), 4.04 (t, J=5 Hz, 64H), 4.40–5.20 (m, 64H), 6.40–7.15 (m, 90H), 7.10–7.40 (m, 4H). MALDI-TOF MS: 9390.0 ([M+Na$^+$] calculated for $C_{508}H_{638}O_{164}Na$: 9391.5). Elemental analysis calculated for $C_{508}H_{638}O_{164}$: C 65.11%, H 6.87%, O 28.02%, found: C 65.01%, H 6.93%, O 28.06%.

4.4. Molecular modeling

The Molecular Dynamics studies have been performed on SGI Origin 200 and Octane^2 workstations using the Discover 3 software from Accelrys (http://www.accelrys.com) with the pcff forcefield. The previously minimized structures were allowed to equilibrate for 500 ps at a 300 K isotherm by the MD simulation (in the NVT ensemble with a time step of 1 fs).

4.5. ESMS

Positive ES mass spectra were obtained on an ES triple quadrupole mass spectrometer Quattro II with a mass-to-charge (m/z) ratio range extended to 8000 (Micromass, Altrincham, UK). The ES source was heated to 45°C. The sampling cone voltage (V_c) was at 160 V to allow the transmission of ions with m/z>4000 without fragmentation processes. Under these conditions, reproducible spectra were also obtained. Sample solutions were introduced into the mass spectrometer source with a syringe pump (Harvard type 55 1111: Harvard Apparatus Inc., South Natick, MA, USA) with a flow rate of 6 μL min^{-1}. Calibration was performed using protonated horse myoglobin. Scanning was performed in the MCA (Multi Channel Analyzer) mode, and several scans were summed to obtain the final spectrum. Samples for ESMS were prepared by dissolving the compound under study in a solution of CH_2Cl_2 containing 1% formic acid to achieve a concentration of 10^{-4} M. After stirring at room temperature for 1 min, the clear red solution was directly analyzed by ESMS.

4.6. MALDI-TOF MS

Mass measurement were carried out on a Brucker BIFLEX™ matrix-assisted laser desorption time-of-flight mass spectrometer (MALDI-TOF) equipped with SCOUT™ High Resolution Optics, an X–Y multi-sample probe and a gridless reflector. Ionization is accomplished with the 337 nm beam from a nitrogen laser with a repetition rate of 3 Hz. All data were acquired at a maximum accelerating potential of 20 kV in the linear positive ion mode. The output signal from the detector was digitized at a sampling rate of 1 GHz. A saturated solution of 1,8,9-trihydroxyanthracene (dithranol ALDRICH EC: 214-538-0) in CH_2Cl_2 was used as a matrix. Typically, a 1/1 mixture of the sample

solution in CH_2Cl_2 was mixed with the matrix solution and 0.5 μL of the resulting mixture was deposited on the probe tip. Calibration was performed in the external mode with insulin (5734.6 Da) and ACTH (2465.2 Da).

4.7. Photophysical measurements

The photophysical investigations were carried out in toluene, dicloromethane, and acetonitrile (Carlo Erba, spectrofluorimetric grade) and toluene-d_8 from Aldrich. The samples were normally placed in fluorimetric 1 cm path cuvettes. Absorption spectra were recorded with a Perkin–Elmer λ40 spectrophotometer. Uncorrected emission spectra were obtained with a Spex Fluorolog II spectrofluorimeter (continuous 150 W Xe lamp), equipped with a Hamamatsu R-928 photomultiplier tube. The corrected spectra were obtained via a calibration curve determined with a procedure described earlier.[55] Fluorescence quantum yields obtained from spectra on an energy scale (cm^{-1}) were measured with the method described by Demas and Crosby[56] using as standard air equilibrated solutions of $[Os(phen)_3]^{2+}$ in acetonitrile (Φ_{em}=0.005).[57]

The steady-state IR luminescence spectra were obtained with an apparatus available at the Chemistry Department of the University of Bologna (Italy) and described in detail earlier.[55] A continuous 450 W Xenon lamp was used as light source, excitation was performed at 480 nm. The determination of the relative yields of singlet oxygen sensitization in a given solvent can be obtained by monitoring the singlet oxygen luminescence intensity at 1268 nm of solutions displaying the same optical density at the excitation wavelength (0.2).[58]

Emission lifetimes in the nanosecond time scale were determined with an IBH single photon counting spectrometer equipped with a thyratron gated nitrogen lamp working in the range 2–40 KHz (λ_{exc}=337 nm, 0.5 ns time resolution); the detector was a red-sensitive (185–850 nm) Hamamatsu R-3237-01 photomultiplier tube.

Transient absorption spectra in the nanosecond–microsecond time domain were obtained by means of a flash-photolysis system described in detail earlier.[59] Excitation was performed with the third harmonic (355 nm) of a Nd:YAG laser (J.K. Lasers Ltd) with 20 ns pulse duration and 1–2 mJ of energy per pulse. Triplet lifetimes were obtained by averaging at least five different decays recorded around the maximum of the absorption peak (680–720 nm). When necessary, oxygen was removed by at least four freeze–thaw-pump cycles by means of a diffusive vacuum pump at 10^{-6} Torr (CH_2Cl_2, PhMe) or by bubbling argon for several minutes through the solution (CH_3CN).

Emission decays of singlet oxygen at 1270 nm were recorded with a liquid nitrogen cooled germanium detector and preamplifier (Applied Detector Corp., Fresno, CA, Mod. 403 HS) connected to a Tektronix 468 digitizer interfaced with a PC. The 1270 nm wavelength was selected with suitable interference filters.

Experimental uncertainties are estimated to be ±7% for UV–VIS emission and transient absorption lifetimes, ±10% for NIR emission lifetimes, ±20% for emission quantum yields, and ±2 nm for absorption and emission peaks, respectively.

Acknowledgements

This work was supported by the CNR, the CNRS and the French Ministry of Research (ACI Jeunes Chercheurs). We thank Professor A. Juris (Department of Chemistry, University of Bologna) for allowing the use of the IR spectrofluorimeter. G. A. thanks Italian MIUR (Progetto 5%) and Y. R. the French Ministry of Research for their fellowships. We further thank L. Oswald and M. Minghetti for technical help. N. A. and A. V. D. are grateful to EU for the TMR contract no. CT98-0226.

References

1. Newcome, G. R.; Moorefield, C. N.; Vögtle, F. *Dendrimers and Dendrons: Concepts, Syntheses, Applications*; VCH: Weinheim, 2001.
2. Balzani, V.; Campagna, S.; Denti, G.; Juris, A.; Serroni, S.; Venturi, M. *Acc. Chem. Res.* **1998**, *31*, 26–34.
3. Frey, H. *Angew. Chem. Int. Ed.* **1998**, *37*, 2193–2197.
4. Archut, A.; Vögtle, F. *Chem. Soc. Rev.* **1998**, *27*, 233–240.
5. Gorman, C. *Adv. Mater.* **1998**, *10*, 295–309.
6. Hearshaw, M. A.; Moss, J. R. *Chem. Commun.* **1999**, 1–8.
7. Newkome, G. R.; He, E. F.; Moorefield, C. N. *Chem. Rev.* **1999**, *99*, 1689–1746.
8. Berresheim, A. J.; Muller, M.; Mullen, K. *Chem. Rev.* **1999**, *99*, 1747–1785.
9. Fischer, M.; Vögtle, F. *Angew. Chem. Int. Ed.* **1999**, *28*, 884–905.
10. Zeng, F. W.; Zimmerman, S. C. *Chem. Rev.* **1997**, *97*, 1681–1712.
11. Chow, H. F.; Mong, T. K. K.; Nongrum, M. F.; Wan, C. W. *Tetrahedron* **1998**, *54*, 8543–8660.
12. Smith, D. K.; Diederich, F. *Chem. Eur. J.* **1998**, *4*, 1353–1361.
13. Bosman, A. W.; Janssen, H. M.; Meijer, E. W. *Chem. Rev.* **1999**, *99*, 1665–1688.
14. Adronov, A.; Frechet, J. M. J. *Chem. Commun.* **2000**, 1701–1710.
15. Inoue, K. *Prog. Polym. Sci.* **2000**, *25*, 453–571.
16. Nierengarten, J. F. *Chem. Eur. J.* **2000**, *6*, 3667–3670.
17. Balzani, V.; Ceroni, P.; Juris, A.; Venturi, M.; Campagna, S.; Puntoriero, F.; Serroni, S. *Coord. Chem. Rev.* **2001**, *219*, 545–572.
18. Grayson, S. K.; Frechet, J. M. J. *Chem. Rev.* **2001**, *101*, 3819–3867.
19. Hecht, S.; Frechet, J. M. J. *Angew. Chem. Int. Ed.* **2001**, *40*, 74–91.
20. Gorman, C. B.; Smith, J. C. *Acc. Chem. Res.* **2001**, *34*, 60–71.
21. Rio, Y.; Accorsi, G.; Nierengarten, H.; Rehspringer, J. L.; Honerlage, B.; Kopitkovas, G.; Chugreev, A.; Van Dorsselaer, A.; Armaroli, N.; Nierengarten, J. F. *New J. Chem.* **2002**, *26*, 1146–1154.
22. Nierengarten, J. F.; Habicher, T.; Kessinger, R.; Cardullo, F.; Diederich, F.; Gramlich, V.; Gisselbrecht, J. P.; Boudon, C.; Gross, M. *Helv. Chim. Acta* **1997**, *80*, 2238–2276.

23. Rio, Y.; Nicoud, J. F.; Rehspringer, J. L.; Nierengarten, J. F. *Tetrahedron Lett.* **2000**, *41*, 10207–10210.
24. Hannon, M. J.; Mayers, P. C.; Taylor, P. C. *J. Chem. Soc., Perkin Trans. 1* **2000**, 1881–1889.
25. Nierengarten, J. F.; Gramlich, V.; Cardullo, F.; Diederich, F. *Angew. Chem., Int. Ed. Engl.* **1996**, *35*, 2101–2103.
26. Bingel, C. *Chem. Ber.* **1993**, *126*, 1957–1959.
27. Nierengarten, J. F.; Felder, D.; Nicoud, J. F. *Tetrahedron Lett.* **1999**, *40*, 269–272.
28. Nierengarten, J. F.; Schall, C.; Nicoud, J. F. *Angew. Chem. Int. Ed.* **1998**, *37*, 1934–1936.
29. Armaroli, N.; Boudon, C.; Felder, D.; Gisselbrecht, J. P.; Gross, M.; Marconi, G.; Nicoud, J. F.; Nierengarten, J. F.; Vicinelli, V. *Angew. Chem. Int. Ed.* **1999**, *38*, 3730–3733.
30. Woods, C. R.; Bourgeois, J. P.; Seiler, P.; Diederich, F. *Angew. Chem. Int. Ed.* **2000**, *39*, 3813–3816.
31. Hirsch, A.; Lamparth, I.; Karfunkel, H. R. *Angew. Chem., Int. Ed. Engl.* **1994**, *33*, 437–438.
32. Jolliffe, K. A.; Calama, M. C.; Fokkens, R.; Nibbering, N. M. M.; Timmerman, P.; Reinhoudt, D. N. *Angew. Chem. Int. Ed.* **1998**, *37*, 1247–1251.
33. Russell, K. C.; Leize, E.; Vandorsselaer, A.; Lehn, J. M. *Angew. Chem., Int. Ed. Engl.* **1995**, *34*, 209–213.
34. Felder, D.; Nierengarten, H.; Gisselbrecht, J. P.; Boudon, C.; Leize, E.; Nicoud, J. F.; Gross, M.; Van Dorsselaer, A.; Nierengarten, J. F. *New J. Chem.* **2000**, *24*, 687–695.
35. Murata, Y.; Ito, M.; Komatsu, K. *J. Mater. Chem.* **2002**, *12*, 2009–2020.
36. Eckert, J. F.; Byrne, D.; Nicoud, J. F.; Oswald, L.; Nierengarten, J. F.; Numata, M.; Ikeda, A.; Shinkai, S.; Armaroli, N. *New J. Chem.* **2000**, *24*, 749–758.
37. Balzani, V.; Ceroni, P.; Gestermann, S.; Gorka, M.; Kauffmann, C.; Vogtle, F. *Tetrahedron* **2002**, *58*, 629–637.
38. Bensasson, R. V.; Bienvenue, E.; Fabre, C.; Janot, J. M.; Land, E. J.; Leach, S.; Leboulaire, V.; Rassat, A.; Roux, S.; Seta, P. *Chem. Eur. J.* **1998**, *4*, 270–278.
39. Armaroli, N. Photoinduced Energy Transfer Processes in Functionalized Fullerenes. In *Fullerenes: From Synthesis to Optoelectronic Properties*; Guldi, D. M., Martin, N., Eds.; Kluwer Academic: Dordrecht, 2002; pp 137–162.
40. Issberner, J.; Vögtle, F.; De Cola, L.; Balzani, V. *Chem. Eur. J.* **1997**, *3*, 706–712.
41. Vögtle, F.; Plevoets, M.; Nieger, M.; Azzellini, G. C.; Credi, A.; De Cola, L.; De Marchis, V.; Venturi, M.; Balzani, V. *J. Am. Chem. Soc.* **1999**, *121*, 6290–6298.
42. Zhou, X. L.; Tyson, D. S.; Castellano, F. N. *Angew. Chem. Int. Ed.* **2000**, *39*, 4301–4305.
43. Birks, J. B. *Photophysics of Aromatic Molecules*; Wiley-Interscience: London, 1970.
44. Schwell, M.; Wachter, N. K.; Rice, J. H.; Galaup, J. P.; Leach, S.; Taylor, R.; Bensasson, R. V. *Chem. Phys. Lett.* **2001**, *339*, 29–35.
45. Kunieda, R.; Fujitsuka, M.; Ito, O.; Ito, M.; Murata, Y.; Komatsu, K. *J. Phys. Chem. B* **2002**, *106*, 7193–7199.
46. Bensasson, R. V.; Schwell, M.; Fanti, M.; Wachter, N. K.; Lopez, J. O.; Janot, J.-M.; Birkett, P. R.; Land, E. J.; Leach, S.; Seta, P.; Taylor, R.; Zerbetto, F. *Chem. Phys. Chem.* **2001**, 109–114.
47. Kordatos, K.; Da Ros, T.; Prato, M.; Leach, S.; Land, E. J.; Bensasson, R. V. *Chem. Phys. Lett.* **2001**, *334*, 221–228.
48. Armaroli, N.; Accorsi, G.; Gisselbrecht, J. P.; Gross, M.; Krasnikov, V.; Tsamouras, D.; Hadziioannou, G.; Gomez-Escalonilla, M. J.; Langa, F.; Eckert, J. F.; Nierengarten, J. F. *J. Mater. Chem.* **2002**, *12*, 2077–2087.
49. Wilkinson, F.; Helman, W. P.; Ross, A. B. *J. Phys. Chem. Ref. Data* **1993**, *22*, 113–262.
50. Darmanyan, A. P.; Arbogast, J. W.; Foote, C. S. *J. Phys. Chem.* **1991**, *95*, 7308–7312.
51. Gorman, A. A.; Krasnovsky, A. A.; Rodgers, M. A. J. *J. Phys. Chem.* **1991**, *95*, 598–601.
52. Scurlock, R. D.; Nonell, S.; Braslavsky, S. E.; Ogilby, P. R. *J. Phys. Chem.* **1995**, *99*, 3521–3526.
53. Schmidt, R.; Brauer, H.-D. *J. Am. Chem. Soc.* **1987**, *109*, 6976–6981.
54. Scurlock, R. D.; Ogilby, P. R. *J. Phys. Chem.* **1987**, *91*, 4599–4602.
55. Armaroli, N.; Marconi, G.; Echegoyen, L.; Bourgeois, J. P.; Diederich, F. *Chem. Eur. J.* **2000**, *6*, 1629–1645.
56. Demas, J. N.; Crosby, G. A. *J. Phys. Chem.* **1971**, *75*, 991.
57. Kober, E. M.; Caspar, J. V.; Lumpkin, R. S.; Meyer, T. J. *J. Phys. Chem.* **1986**, *90*, 3722–3734.
58. Wirp, C.; Gusten, H.; Brauer, H. D. *Ber. Bunsen-Ges. Phys. Chem.* **1996**, *100*, 1217–1225.
59. Flamigni, L. *J. Phys. Chem.* **1992**, *96*, 3331–3337.